



## Luminescence of brown CVD diamond: 468 nm luminescence center

A.M. Zaitsev<sup>a,b,\*</sup>, N.M. Kazuchits<sup>c</sup>, K.S. Moe<sup>b</sup>, J.E. Butler<sup>d</sup>, O.V. Korolik<sup>c</sup>, M.S. Rusetsky<sup>c</sup>, V.N. Kazuchits<sup>c</sup>

<sup>a</sup> The College of Staten Island/CUNY, 2800 Victory Blvd., Staten Island, NY 10312, USA

<sup>b</sup> Gemological Institute of America, 50 W 47th St #800, New York, NY 10036, USA

<sup>c</sup> Belarusian State University, Nezavisimosti Ave. 4, 220030 Minsk, Belarus

<sup>d</sup> Cubic Carbon Ceramics, 855 Carson Road, Huntingtown, MD 20639, USA

### ARTICLE INFO

#### Keywords

CVD diamond  
Brown color  
Center 468 nm

### ABSTRACT

Detailed study of the luminescence of multiple brown CVD diamonds was performed. It has been found that the well-known optical center with zero-phonon line at 468 nm is a characteristic of brown color. It has been found that the defects responsible for 468 nm center are located within brown striations suggesting close relation of the 468 nm center and the vacancy clusters. Simultaneous reduction of the intensity of 468 nm center and brown color during annealing support the assumption of their close relation. Identical spectroscopic parameters of the 468 nm center and the radiation center with ZPL at 492 nm suggest that the former relates to an intrinsic defect probably containing vacancies. The distribution of intensity of the 468 nm center in some brown diamonds follows the distribution of the NV<sup>-</sup> center while being opposite to that of the NV<sup>0</sup> center and the dislocation-related A-band. This observation suggests the negative charge state of the 468 nm center. Due to its high luminescence efficiency, the 468 nm center can be used as a highly sensitive indicator of the traces of vacancy clusters. We found that the 468 nm center is detected practically in every as-grown CVD diamond including colorless CVD diamonds of high structural perfection and high purity.

### 1. Introduction

Common color of natural diamond is brown. Brown color is also common component for as-grown CVD diamond. However, brown color is not a characteristic of the diamond crystal, but the manifestation of its imperfect crystal structure. For many applications, including jewelry, optics, electronics and medicine, the brown color is a feature downgrading the quality of diamond. This is why the reduction of brown color (and eventually removal) and the development of the technologies of growth of colorless CVD diamond attract attention of academic and practical diamond growers.

For many natural brown diamonds including low-nitrogen type IIa diamonds, the origin of their color is large vacancy aggregates (vacancy clusters) [1]. For brown CVD diamonds, the origin of brown color is likely the same [2]. Although visually the brown color of natural diamonds is similar to that of CVD diamonds, the thermodynamic and spectroscopic characteristics of the defects responsible for brown color in natural and CVD diamonds differ. The temperature stability of the brown color in CVD diamonds may range from 1600 to 1800 °C [2,3], which is lower than in natural diamonds (over 2100 °C [4,5]). The optical absorption features of natural and CVD brown diamonds are dif-

ferent too. Brown color is caused by a continuous absorption over the whole visible spectral range with intensity gradually increasing from infrared to ultraviolet. Two broad absorption bands with maxima at wavelengths of 360 and 550 nm frequently seen in the spectra of brown natural diamonds are believed to closely relate to brown color [5]. Similar absorption spectrum consisting of the continuum and two broad bands is characteristic for brown CVD diamonds. However, in brown CVD diamonds, the spectral position of the broad bands is shifted to wavelengths of 380 nm and 520 nm respectively [3,6,7]. These differences raise the question of whether the vacancy clusters in natural and CVD diamonds are of the same structure [2,8]. A suggestion was made that the vacancy clusters in natural diamonds are globular 3D nano-cavities while in CVD diamond they are preferentially 2D vacancy discs oriented along (111) and/or (110) planes [8]. In [9] it was argued that this difference is not necessarily the form, but the size. Much shorter growth time of CVD diamonds than natural diamonds can limit the diffusion of vacancies and, consequently, the vacancy clusters in CVD diamonds are expected to be smaller. This supposition is in agreement with the results of [2], where it was concluded that in CVD brown diamonds annealing makes vacancy clusters larger. It was also found that the concentration of small vacancy clusters reduces with an-

\* Corresponding author at: The College of Staten Island/CUNY, 2800 Victory Blvd., Staten Island, NY 10312, USA.

E-mail address: [alexander.zaitsev@csi.cuny.edu](mailto:alexander.zaitsev@csi.cuny.edu) (A.M. Zaitsev)

nealing. A conclusion was made that only small-size vacancy clusters are optically (absorption) active.

The presence of brown color is seen visually and its intensity can be evaluated from the optical absorption measurements. Although the optical absorption is the direct method for the quantitative analysis of color, it has some limitations. For correct quantitative measurements of optical absorption, the sample must be of a required shape and its surface must be well-polished. The reliable absorption measurements also require rather large sample volumes: sampled area and thickness. Besides, the sensitivity of the optical absorption method is low when measuring broad spectral features. These limitations may make one to look for alternative optical methods suitable for the measurements of brown color in very small samples and in samples of irregular shape, or new methods for detection of faint brown color.

A complementary optical technique to optical absorption is luminescence. Luminescence methods can be used for measurements of samples practically of any shape and size. In terms of sensitivity, the luminescence methods, in particular photoluminescence (PL), surpass optical absorption by many orders of magnitude being capable of the measurements of single photons emitted by individual defects. Unfortunately, no luminescence feature or center has been identified yet as directly related to the defects responsible for the brown color, although numerous luminescence centers have been reported in luminescence spectra of brown CVD diamonds (for references see [10]). Most of these luminescence centers are features of natural diamond only. In brown CVD diamonds, no luminescence center has been ascribed to brown color too.

In this communication we report the results of spectroscopic studies of the luminescence center with zero-phonon line (ZPL) at a wavelength of 467.7 nm at liquid nitrogen temperature (LNT), which is one of the most common and specific optical center of brown CVD diamond. From now on we will refer to this center as 468 nm center. We have found that 468 nm center is closely related to vacancy clusters and its intensity can be used as a measure of the presence of brown color.

## 2. Experimental

### 2.1. Samples

Several single crystal CVD diamond samples grown in GIA CVD Diamond Lab were studied in this research. High vacuum PLASSYS 150 2.45 GHz microwave plasma reactor was used. All samples were grown on (100)-oriented single crystal synthetic diamond seeds of size  $7 \times 7 \times 0.3 \text{ mm}^3$  in a  $\text{H}_2/\text{CH}_4$  gas mixture (methane content from 4 to 6%) at pressure ranging from 300 to 360 mbar and gas flow rate ranging from 100 to 200 sccm. The purity of the gasses used was at a level of 10 ppm (commercial ultra-high purity grade). All samples were grown at a temperature of 950 °C at a microwave power from 3.5 to 4 kW. For some of them, nitrogen was added to the gas mixture. The samples were grown in several steps to a total thickness of 3 to 4 mm. Three samples (#032091, #305293 and #304017) were grown on seeds placed horizontally in the center of the seed holder. Thus, the growth conditions were nominally uniform over the growing diamond

surface. One sample (#304023) was grown with the seed placed at an angle with respect to the plasma front. The as-grown diamond blocks were cross-sectionally cut in plates along vertical (100) plane and then polished from both sides.

Samples #032091 and #304017 were grown on CVD seeds without addition of nitrogen to the growth gas. Interior of the sample #032091 was very included. However, one cross-sectional slice made of this sample had no inclusions protruding to the surface. This slice was used for the mapping of the photoluminescence intensity of 468 nm center and A-band. Sample #304017 had less inclusions and revealed very non-uniform distribution of brown color. Sample #305293 was grown on CVD seed in 6 layers with nitrogen addition gradually increasing from the first to the sixth layer. Detailed information on the growth conditions of this sample can be found in [9].

Sample #304023 was grown on HPHT diamond seed in three layers to a total thickness of 3.25 mm. No nitrogen was added during growth. The first layer of this sample was grown with the seed placed on a beveled holder at an angle of 15° off the horizontal (Fig. 1a).

With this position of the sample, the growth surface was exposed to plasma nonuniformly and the growth rate over the sample surface was nonuniform too. The area closer to plasma grew faster than the distant area. After the growth of the first layer, the sample was turned by 180° and the second layer was grown (Fig. 1b). Since the growth conditions over the growth surface were reversed, after the second growth the sample had approximately equal thickness over its area. The third layer was grown with the sample placed horizontally under plasma (Fig. 1c). The first and second layers revealed massive formation of growth steps and brown striations (Fig. 1d). We assume that the tilted position of the seed and non-uniform growth was the condition provoking the formation of brown striations. The third layer grew near colorless.

Two slices of the sample #305293 were annealed. One of them was annealed in vacuum at a temperature of 1700 °C for 10 min (LPHT annealing). Another one was annealed at a temperature 1880 °C and a pressure of 52 kbar for 4 h (HPHT annealing) in a BARS high pressure apparatus.

### 2.2. Measurements

PL measurements were performed using spectrometers Nanofinder High End (LOTIS TII Tokyo Instruments) combined with a 3D scanning confocal microscope at temperatures from 30 to 500 K and Renishaw inVia Raman confocal microscope at liquid nitrogen temperature (LNT). Most measurements were performed with laser excitation at wavelengths 354.8 nm. For some measurements, the excitation at wavelengths 324.8, 457.0, 473, 532, 633 and 830 nm were used too.

Distribution of intensity of luminescence centers over sample area (photoluminescence mapping) was obtained at LNT with scanning Raman microscope Thermo DXRxi.

DiamondView instrument (illumination wavelengths <230 nm) with blue filter was used for mapping the intensity of A-band luminescence. Fluorescence images of brown striations were taken with Nikon Eclipse Ti inverted microscope equipped with mercury lamp for UV excitation and broad band optical filter.

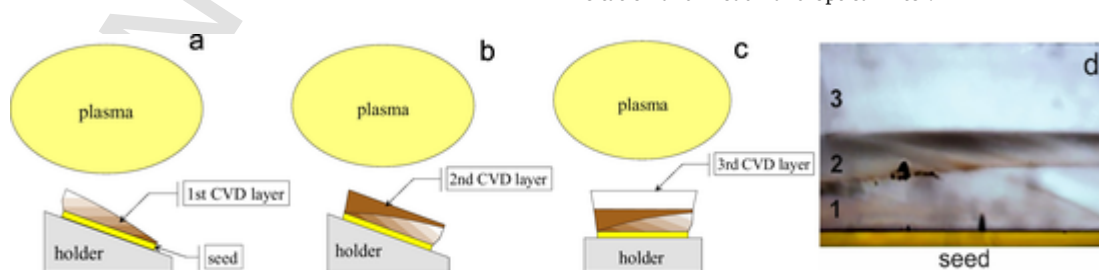


Fig. 1. (a, b, c) Schematics showing position of sample #304023 during growth. The area of the sample closer to plasma is growing faster than the more distant area. (d) Image of a plate cross-sectionally cut of this sample. Massive formation of brown striations is seen in the layers 1 and 2 grown on beveled holder. The 3rd layer grown horizontally reveals no brown striations.

### 3. Experimental results

#### 3.1. Imaging and PL mapping

All samples studied in this research had intense brown striations similar to those reported in a number of publications and in our recent paper (e.g. [6,9]). In the images of the cross-sectionally cut plates, these striations are seen propagating either parallel to the growth surface, or tilted to an angle from 10 to 20° with respect to the growth surface (Figs. 1, 2, 3). When comparing the optical and fluorescence images it was found that the brown striations produce enhanced green luminescence (Figs. 2, 3).

Distributions of PL intensity of the centers 468 nm, NV<sup>0</sup>, NV<sup>-</sup> (obtained with the scanning Raman microscope) and A-band (DiamondView imaging) are shown in Fig. 3. It is seen that the luminescence of the 468 nm center is stronger in the areas of brown striations. In some samples, the intensity of 468 nm center follows two distinctive patterns crossing each other: the pattern of brown striations and a pattern of stripes propagating in the directions close to the direction of diamond growth (“vertical” striations) (Fig. 3c). The angle between the brown striations and the growth surface is either 0° or about 17°, while the angle between the “vertical” striations is either 90° or about 16° with respect to the growth surface (Fig. 3c).

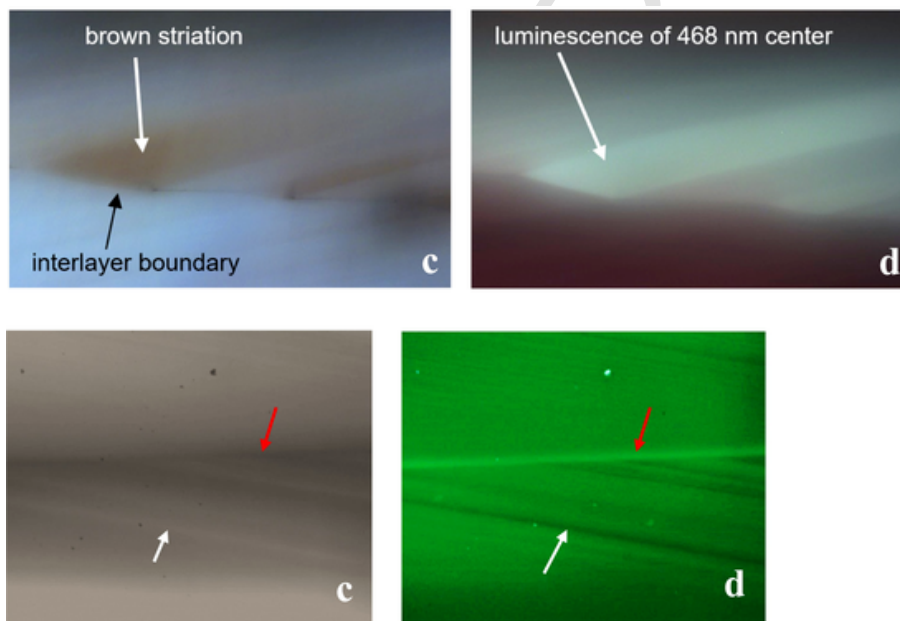


**Fig. 2.** Comparison of optical images (left) with fluorescence images (right) taken with fluorescence microscope. Darker stripes in optical images are brown striations. Green color in luminescence images is due to luminescence of the 468 nm center. All areas of darker brown color produce brighter green luminescence. (a, b) Brown striations are initiated at terrace edges of sample #304023. (c, d) Interlayer boundary of dark brown color and tilted brown striations in the sample #304017 produce strong green luminescence (shown with red arrows). White arrows show near-colorless stripe between tilted brown striations. This stripe has low intensity of the green luminescence.

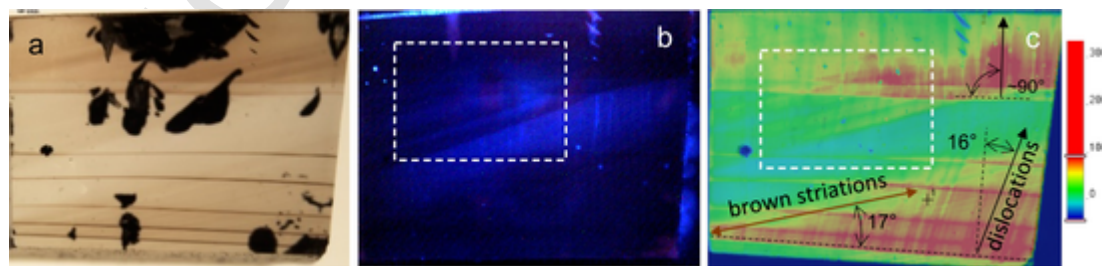


**Fig. 3.** Optical image (a), distribution of PL intensity of the A-band (b) and distribution of PL intensity of 468 nm center (c) over the surface of the sample #032091. The large black inclusions are not protruding to the sample surface. Brown arrow in (c) shows direction of propagation of brown striations. Black arrow shows direction of propagation of “vertical” striations. The bar on the right is the color scale of PL intensity measured at wavelength 468 nm for image (c). Dashed lines show the directions parallel and perpendicular with respect to the growth surface.

DiamondView image of sample #032091 shows distribution of the luminescence intensity of A-band (Fig. 3b). It is seen that in general the A-band distribution is opposite to the intensity distributions of the brown color and 468 nm center. The areas of high intensity of the 468 nm center correspond to the areas of low intensity of the A-band (shown with dashed white rectangles in Fig. 3b,c).

The patterns of the distribution of intensity of the centers 468 nm, NV<sup>-</sup> and NV<sup>0</sup> are compared in Fig. 4b,c,d. It is seen that the intensity of 468 nm center follows the intensity of NV centers. This tendency is better for NV<sup>-</sup> center than for NV<sup>0</sup> center. In some parts of the diamond (Fig. 3) the 468 nm PL tends to be strong when the NV<sup>-</sup> PL is strong. In those regions, the PL from NV<sup>0</sup> centers and from the dislocation-related A-band tends to be weak.

Although in general the distribution of the 468 nm center follows the distribution of the NV centers, there are places where they exhibit different distributions.

#### 3.2. Spectra of 468 nm center

Photoluminescence measurements were performed on many samples. We found no qualitative differences between the spectra. They all exhibited essentially the same set of optical centers the dominating being NV<sup>-</sup>, NV<sup>0</sup>, 533 nm and 468 nm centers. However, the relative in-

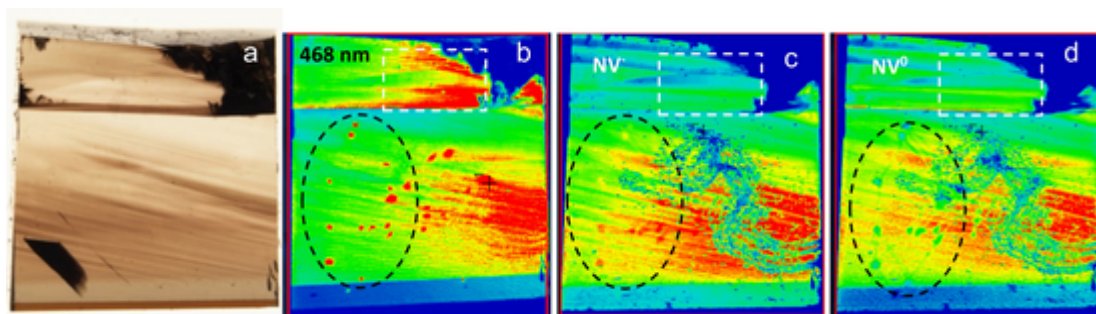


Fig. 4. Optical image (a) and distribution of PL intensity of the centers 468 nm (b),  $NV^-$  (c) and  $NV^0$  (d) over the sample #304017. Dashed ovals mark multiple spots where the 468 nm and  $NV^-$  centers have high intensity, while  $NV^0$  center has low intensity. Dashed rectangles show the area where the intensity of 468 nm center does not follow closely the intensity of  $NV^-$  centers.

tensity of 468 nm center was always much stronger in dark brown areas than in light brown and near colorless areas (Fig. 5).

A complex broad band in the spectral range 850–1000 nm is excited with 830 nm laser. Intensity of this band well correlates with the intensity of 468 nm center. This band can be very strong in dark brown areas. We have found that the 830 nm band and several minor accompanying lines (not shown) are Raman scattering on vacancy clusters. The research results on these Raman features will be reported elsewhere.

PL intensity of the 468 nm center depends on the excitation wavelength. When excited at wavelength 457 nm, the center can be two or-

ders of magnitude stronger than when excited at wavelength 325 nm. The 468 nm center is also active in cathodoluminescence (CL) (Fig. 6). The efficiency of its excitation in CL and with UV lasers (325 and 355 nm) is comparable with that of  $NV^0$  center (Fig. 6a).

The spectrum of 468 nm center is rather simple (Fig. 6b). It consists of sharp zero-phonon line (ZPL) at wavelength 467.7 nm (at LNT) and several equidistant vibrational replicas spaced 73 meV apart from each other. This spectrum coincides very closely with the spectrum of the radiation center with ZPL at 492 nm [11] (Fig. 6b). Both centers interact predominantly with vibrations of energy 73 meV. Phonon den-

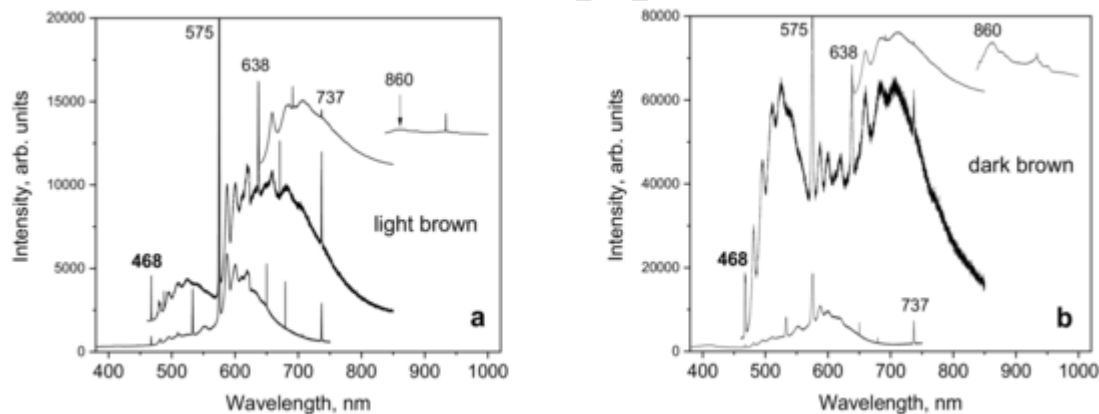


Fig. 5. PL spectra taken with lasers of wavelengths 325, 457, 633 and 830 nm from low-nitrogen light brown area (a) and high-nitrogen dark brown area (b) of sample #305289. Intensities of spectra in both graphs are adjusted to equal intensity of diamond Raman line. Note 4-fold greater scale of vertical axis of graph (b). All spectra were taken at LNT.

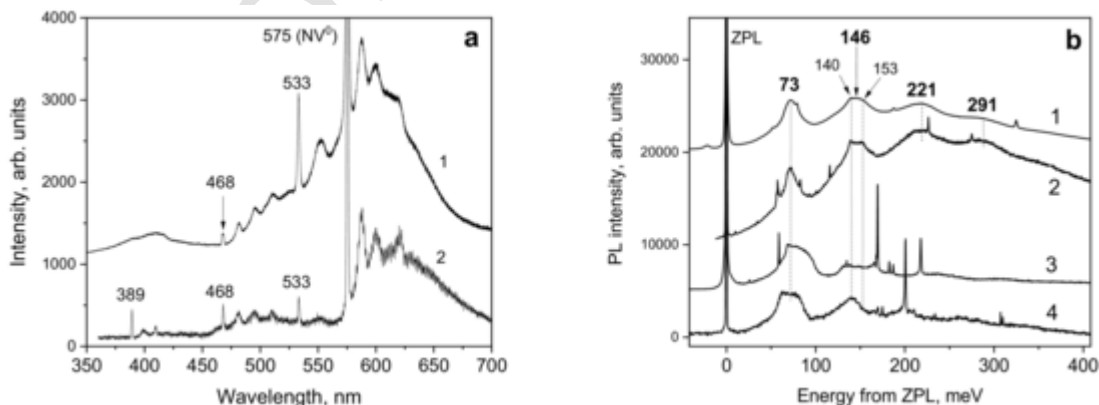


Fig. 6. (a) Comparison of PL (1) and CL (2) spectra of 468 nm center taken from brown areas of two samples grown with equal concentration of nitrogen in growth gas. PL was excited with 325 nm laser. (b) Comparison of the spectrum of 468 nm center (1) taken from brown CVD diamond with the spectra of 492 nm center (2), TR12 center (3) and 3H center (4) taken from near-colorless CVD diamond irradiated with 1 MeV electrons. Intensities of the spectra of 468 nm and 492 nm centers are adjusted to equal magnitude of their ZPLs.

sity of states of diamond lattice at energies below 80 meV is low and has no distinctive maxima (e.g. [10]). Thus, we believe that the 73 meV vibrations are not lattice phonons, but quasilocal vibrations. Only two very weak features with energies 140 and 153 meV seen on the background of the second vibronic replica in spectra of both centers can be ascribed to the interaction with lattice phonons. In [12], the 468 nm center and TR12 center are discussed as spectroscopically similar and therefore closely related. In Fig. 6b we compare the spectra of the centers 468 nm and TR12. We found that the electron-phonon spectra of these centers differ substantially in shape, energy and the relative strength of the vibronic transitions. We also found that the 3H center, which always accompanies TR12 center, is not a close match to 468 nm center too. In a future communication, we will report that TR12 and 3H centers have closer relation to the 533 nm center of CVD diamonds.

The 468 nm center has a doublet ZPL with lines at wavelengths 468 nm (strong) and 464 nm (weak). The energy difference between them is 20.7 meV. With temperature, the ratio of the intensities  $I_{464}/I_{468}$  of these lines is growing and can be well approximated by the Boltzmann function with activation energy 20.7 meV (Fig. 7a). We found that the 492 nm center has also doublet ZPL. The corresponding lines are at wavelengths 492 nm (strong) and 489.2 nm (weak). The energy difference between the lines is 14.8 meV.

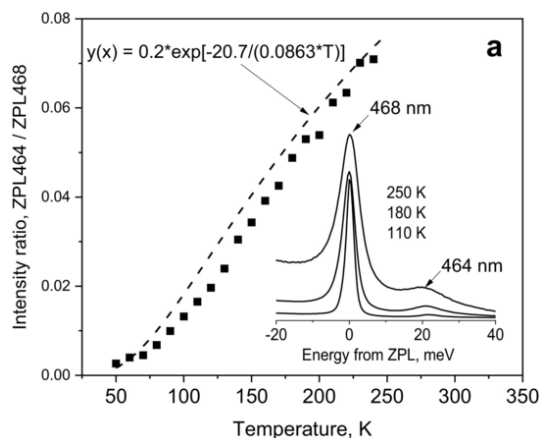


Fig. 7. (a) Temperature dependence of the intensity ratio  $I_{464}/I_{468}$  of the lines 464 nm and 468 nm. Dashed curve is the Boltzmann function for activation energy 20.7 meV. Inset shows the spectra of the lines measured at temperatures 110, 180 and 250 K. (b) PL spectra of 468 nm center taken at room temperature from sample #305293 in as-grown state (1), after LPHT annealing in vacuum at a temperature of 1700 °C (2) and after HPHT annealing at a temperature 1880 °C (3). 468 nm center is not detected after HPHT annealing.

The 468 nm center has a high temperature stability (Fig. 7b). Although annealing reduces its intensity, the center stands heating at temperatures of at least 1700 °C. Annealing at high pressure and high temperature performed at 52 kbar and 1880 °C for 4 h destroys 468 nm center beyond detection limit. This HPHT annealing also eliminates brown color. From our experience, the 468 nm center remains detectable after annealing only if brown color is not removed completely.

At temperatures above 100 K, the spectra taken from brown and near-colorless areas are qualitatively similar. At lower temperatures, the difference becomes substantial. In spectra of near-colorless areas, a very complex band with numerous narrow lines on its background rises in a spectral range from about 470 to 520 nm (Fig. 8a). Relative intensity on this band and the narrow lines decrease fast as temperature goes up. Traces of these features can be seen in the spectra of brown areas too at low temperature (Fig. 8b).

#### 4. Discussion

Preferential localization of the defects responsible for the 468 nm center within brown striations suggests that these defects relate to brown color of CVD diamonds and, consequently, to vacancy clusters. Simultaneous reduction, and eventual disappearance, of brown color and 468 nm center after high temperature annealing support this conclusion. Defects located in the proximity of vacancy clusters or even directly on the walls of vacancy clusters could be a possibility.

As to the atomic structure of these defects, the available information is not sufficient to propose a reasonable model. The fact that the intensity of the 468 nm center follows the intensity of the NV centers may make one to suggest the involvement of nitrogen atoms. However, we think that such a conclusion can be misleading at this point. Firstly, the similarity in the distribution patterns of the 468 nm and NV centers is not perfect. There are areas where the intensity of 468 nm center is very strong but NV centers are rather weak. Secondly, the observed similarity could be merely a consequence of the correlation of the efficiency of nitrogen doping and the intensity of brown color in CVD diamonds [9].

In some brown CVD diamonds the intensity distribution of the 468 nm center is similar to the distribution of the  $NV^-$  center while it is opposite to that of the  $NV^0$  center. This suggests that the 468 nm center may relate to negatively-charged defects. Assuming the negative charge state of the 468 nm center, its enhanced intensity in brown striations can be interpreted as the result on the presence of high concentration of nitrogen donors. This interpretation is in agreement with the anticorrelation of the intensities of 468 nm center and A-band. It is known that the A-band (maximum at about 430 nm) seen in luminescence spectra of low-nitrogen diamonds relates to dislocations [13]. It was shown that the dislocations in diamond act as acceptor-like defects

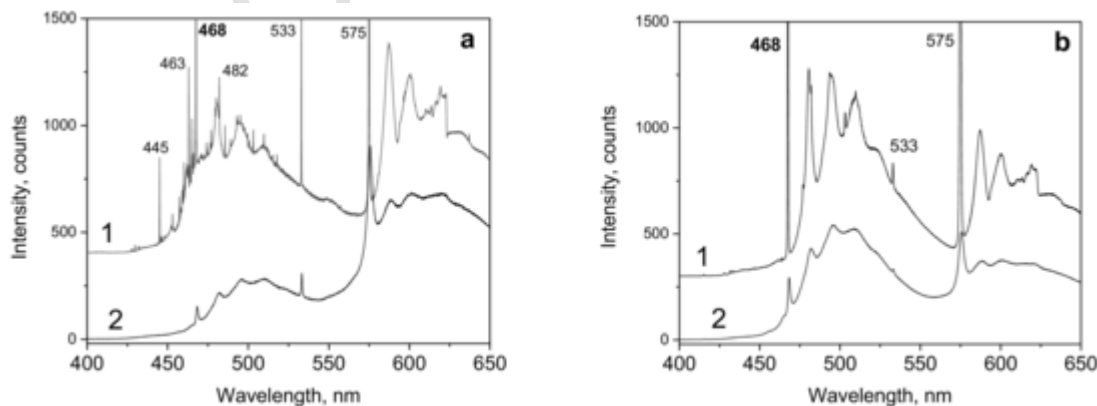


Fig. 8. PL spectra taken at temperatures 30 K (1) and 295 K (2) from near-colorless (a) and brown (b) areas of sample #305293. The strongest ZPLs are labeled. Intensities of the spectra are adjusted to equal intensity of Raman line.

[14]. Thus, the presence of dislocations must suppress the luminescence of negatively charged optical centers.

In [6] it is reported that in single crystal CVD diamonds grown on (100)-oriented substrates the dislocations propagate along directions approximately parallel to the  $\langle 001 \rangle$  growth direction (vertical with respect to the growth surface). The deviation of the dislocation lines from exact  $\langle 001 \rangle$  vertical direction is caused by terraced growth [15]. Our results support this conclusion. As it is seen in Fig. 3c, the angle between the growth plane and the brown striations is about the same as the angle between the “vertical” striations and the vertical  $\langle 001 \rangle$  direction. Thus, the “vertical” striations in the distribution of 468 nm center are the “negative luminescence imprint” of the dislocation bundles formed along the growth direction of CVD diamond. The 468 nm center emission is stronger between the dislocation bundles.

The very close coincidence of the spectra of 468 nm center and the radiation center with ZPL at 492 nm is an indication that the defects responsible for these centers have identical components in their atomic structures. Since 492 nm center is readily created by electron irradiation in any diamond, including high purity quantum grade CVD diamonds, it definitely belongs to an intrinsic defect. Therefore, we think that the 468 nm center also relates to an intrinsic defect rather than to an impurity one. It could be that both centers belong to defects with the same atomic structure. These defects, when surrounded by regular diamond lattice, produce 492 nm center. If they are located at vacancy clusters, their electronic energy levels shift and they produce 468 nm center.

The spectral shift of 468 nm center from the position of 492 nm center by 129 meV due to the interaction with vacancy clusters has probably the same nature as the shift of N3 center by 73 meV from 415 nm to 405 nm when the N3 defects get trapped by pink lamella in natural diamonds [16]. In both cases the shift is towards shorter wavelengths. Spectral shifts of N3 center in natural type IaB diamonds with platelets from 415 nm to 461 nm (the N3a center) and from 415 nm to 540 nm (N3b center) were reported decades ago in [17] and explained as the narrowing of the diamond bandgap in the vicinity of large macroscopic defects with regular atomic structure. We can follow this explanation and assume that the vacancy clusters in brown diamonds also change the diamond bandgap in their vicinity.

Relatively large energy of the quasi-local vibrations interacting with 468 nm center (73 meV) is another hint at its negative charge state. In diamond, the centers originating from negatively charged defects tend to interact with more energetic quasilocal vibrations as compared with the quasilocal vibrations of their neutral counterparts. For instance, negatively charged centers H2, ND1 and NV<sup>-</sup> interact with vibrations of energy 70, 80 and 64 meV respectively. Correspondingly, their neutral counterparts H3, GR1 and NV<sup>0</sup> interact with vibrations of energy 41, 41 and 45 meV. A simple explanation of this tendency is that the greater number of electrons forming the electron orbitals of negatively-charged defects could result in stronger interatomic bonding.

The similarity of the centers 492 nm and 468 nm is also in their doublet ZPL. For the 468 nm center, the two lines of this doublet have wavelengths of 463.9 nm (minor component) and 467.7 nm (major component) at LNT. The energy difference between the lines is 20.7 meV. With temperature, the intensity ratio of the lines  $I_{464}/I_{468}$  is growing and is well approximated by Boltzmann exponential function with the activation energy of 20.7 meV suggesting that the splitting of the electronic transition occurs in the excited state. ZPLs of the 492 nm center are at wavelengths 492 nm (major) and 489.2 nm (minor). We did not have chance to prove thermalization of these lines, but the correlation of their intensities measured in many samples suggests that they belong to one and the same center.

Common components constituting the defects responsible for 492 nm and 468 nm centers could be interstitials and/or vacancies, or both. In case of the 492 nm center, they are produced by irradiation. In case of the 468 nm center, they can be delivered by vacancy clusters. We assume that vacancies are a more probable option. Very different

temperature stability of 492 nm center (completely anneals out at temperatures below 1000 °C [11]) and 468 nm (stands annealing at temperature 1700 °C) can be explained by their very different surrounding. The 492 nm center surrounded by regular crystal lattice may freely diffuse itself and it is open for the interaction with other defects which are mobile during annealing. The 468 nm center being stuck at vacancy cluster does not move itself and is protected from approach by other mobile defects from regular crystal matrix.

Natural brown diamonds have a number of luminescence centers with ZPLs close to wavelength 468 nm [10, 18]. However, none of them has been found to be the same as the 468 nm center of brown CVD diamonds. This suggests that there are factors making vacancy clusters in natural diamonds and in CVD diamonds substantially different. One of these factors could be the hydrogen used for CVD diamond growth. One can assume that the vacancy clusters in CVD diamonds are decorated with hydrogen. Then the interaction with the hydrogen-filled vacancy clusters could be the reason of the unique formation of 468 nm center in CVD diamonds. However, putting forward this assumption, we are not inclined to think that hydrogen atoms are direct constituents of the defects responsible for 468 nm center.

## 5. Conclusion

We performed a detailed study of the 468 nm luminescence center characteristic of brown CVD diamonds. A part of the results related to the spectroscopic characteristics of this center are reported in this communication. Based on these results we make a conclusion that 468 nm center is produced by intrinsic defects in negative charge state. These defects may contain vacancies and they are close analog of the defects responsible for the intrinsic radiation center with ZPL at 492 nm.

Practical importance of the 468 nm center is that its intensity follows the intensity of brown color. Thus, this center can be used as an indicator of the presence of brown color and consequently vacancy clusters in CVD diamonds. Since the luminescence efficiency of the 468 nm center is very high, the center is suitable for detection of trace concentrations of vacancy clusters. From our experience, even CVD diamond of very high structural perfection and high purity reveal the presence of 468 nm center. Only the HPHT annealing, which eliminates brown color, can completely destroy this center.

## Declaration of competing interest

The authors A. M. Zaitsev, N. M. Kazuchits, K. S. Moe, J. E. Butler, O. V. Korolik, M. S. Rusetsky and V. N. Kazuchits of the manuscript **Luminescence of brown CVD diamond: 468 nm luminescence center** declare no conflict of interests.

## Acknowledgements

The authors are grateful to Dr. W. Wang for discussions and A. Chan for preparation of samples.

## References

- [1] L.S. Hounscome, R. Jones, P.M. Martineau, D. Fisher, M.J. Shaw, P.R. Briddon, S. Öberg, Origin of brown coloration in diamond, *Phys. Rev. B* 73 (2006) 125203, doi:10.1103/PhysRevB.73.125203.
- [2] J.M. Maki, F. Tuomisto, C. Kelly, D. Fisher, P.M. Martineau, Effects of thermal treatment on optically active vacancy defects in CVD diamonds, *Phys. B Condens. Matter* 401 (2007) 613–616, doi:10.1016/j.physb.2007.09.034.
- [3] R.U.A. Khan, B.L. Cann, P.M. Martineau, J. Samartseva, J.J.P. Freeth, S.J. Sibley, C.B. Hartland, M.E. Newton, H.K. Dhillon, D.J. Twitchen, Colour-causing defects and their related optoelectronic transitions in single crystal CVD diamond, *J. Phys. Condens. Matter* 25 (2013) 275801, doi:10.1088/0953-8984/25/27/275801.
- [4] J.-M. Maki, F. Tuomisto, C.J. Kelly, D. Fisher, P.M. Martineau, Properties of optically active vacancy clusters in type IIa diamond, *J. Phys. Condens. Matter* 21 (2009) 364216, doi:10.1088/0953-8984/21/36/364216.

- [5] D. Fisher, S.J. Sibley, C.J. Kelly, Brown colour in natural diamond and interaction between the brown related and other colour-inducing defects, *J. Phys. Condens. Matter* 21 (2009) 364213, doi:10.1088/0953-8984/21/36/364213.
- [6] P.M. Martineau, S.C. Lawson, A.J. Taylor, S.J. Quinn, D.J.F. Evans, M.J. Crowder, Identification of synthetic diamond grown using chemical vapor deposition (CVD), *Gems & Gemol.* 40 (2004) 2–25.
- [7] W. Wang, M.S. Hall, K.S. Moe, J. Tower, Th.M. Moses, Latest-generation CVD-grown synthetic diamonds from Apollo Diamond Inc, *Gems & Gemol.* 43 (2007) 294–312.
- [8] R. Jones, Dislocations, vacancies and the brown colour of CVD and natural diamond, *Diam. Relat. Mater.* 18 (2009) 820–826, doi:10.1016/j.diamond.2008.11.027.
- [9] A.M. Zaitsev, N.M. Kazuchits, V.N. Kazuchits, K.S. Moe, M.S. Rusetsky, O.V. Korolik, Kouki Kitajima, J.E. Butler, W. Wang, Nitrogen-doped CVD diamond: nitrogen concentration, color and internal stress, *Diam. Relat. Mater.* (2020) 107794, doi:10.1016/j.diamond.2020.107794.
- [10] A.M. Zaitsev, *Optical Properties of Diamond: A Data Handbook*, Springer Publishing House, Berlin-Heidelberg-New York, 2001, doi:10.1007/978-3-662-04548-0.
- [11] K. Yakubovskii, G.J. Adriaenssens, Optical studies of some interstitial-related centers in CVD diamond, *Phys. Status Solidi (a)* 181 (2000) 59–64, doi:10.1002/1521-396X(200009)181:1 <59::AID-PSSA59>3.0.CO;2-D.
- [12] N. Yamamoto, J.C.H. Spence, D. Fathy, Cathodoluminescence and polarization studies from individual dislocations in diamond, *Philos. Mag. B* 49 (1984) 609–629, doi:10.1080/13642818408227648.
- [13] S.N. Samsonenko, N.D. Samsonenko, Dislocation electrical conductivity of synthetic diamond films, *Semiconductors* 43 (2009) 594–598, doi:10.1134/S1063782609050091.
- [14] P.M. Martineau, M. Gaukroger, R. Khan, D. Evans, Effect of steps on dislocations in CVD diamond grown on {001} substrates, *Phys. Status Solidi (a)* 6 (2009) 1953–1957, doi:10.1002/pssc.200881465.
- [15] E. Gaillou, J.E. Post, N.D. Bassim, A.M. Zaitsev, T. Rose, M.D. Fries, R.M. Stroud, A. Steele, J.E. Butler, Spectroscopic and microscopic characterizations of color lamellae in natural pink diamonds, *Diam. Relat. Mater.* 19 (2010) 1207–1220, doi:10.1016/j.diamond.2010.06.015.
- [16] E.V. Sobolev, A.P. Yeliseev, Thermally stimulated luminescence and phosphorescence of natural diamonds at low temperatures, *J. Struct. Chem.* 17 (1976) 799–801 (Translated from *Zhurnal Strukturnoi Khimii*, Vol. 17, No. 5, pp. 933–935, September–October, 1976 (in Russian)), doi:10.1007/BF00746027.
- [17] B. Dischler, *Handbook of Spectral Lines in Diamond. Volume 1: Tables and Interpretations*, Springer, 2012, doi:10.1007/978-3-642-22215-3.